

Received: 03 December 2018 / Accepted: 10 October 2019 / Published online: 20 December 2019

*electrohydraulics,
valve, drive,
smart materials*

Andrzej MILECKI^{1*}

Dominik RYBARCZYK¹

INVESTIGATIONS OF APPLICATIONS OF SMART MATERIALS AND METHODS IN FLUID VALVES AND DRIVES

In the paper the investigations performed at the Division of Mechatronic Devices at Poznan University of Technology in the area of application of both: smart materials in electro-hydraulic and electro-pneumatic valves, and new methods to control of hydraulic servo drives, are presented. In a first part the piezo bender actuator is shortly described and its application in servo valve is proposed. This actuator replaced the torque motor in the available on the market servo valve. The new valve simulation model is proposed. The simulation and investigations results of the servo valve with the piezo bending actuator are included. In the next part of the paper the application of piezo tube actuator in flapper-nozzle pneumatic valve is described. The test stand and investigations results are presented. Later, in the article, the Model Following Control (MFC) and Fractional order Control (FoC) methods are described. Their application in control of electrohydraulic servo drive is proposed. Some investigations results are included in the paper, showing the advantages of those control methods.

1. INTRODUCTION

In this paper the chosen investigation results made at Division of Mechatronic Devices at Poznan University of Technology (PUT) are described. At first, the applications of so called “smart” materials in electrohydraulic valves are presented. Such materials are sometimes called also as intelligent. They have itself made it possible to develop the mechatronic actuators without moving parts, which are typical in electric motors or electromagnets. These materials support the general mechatronic concept of integration of smart mechanical drives with intelligent controllers. The smart materials are mainly: piezo actuators, different shape memory alloys, electro- and magneto-rheological fluids and elastomers, as well as pneumatic muscles and smart fabrics. The oldest “smart” material is the piezoelectric element, which may be used as actuator, converting electrical signal into mechanical deformation. Piezoelements are characterized by fast response, but their displacement is low. These actuators may be applied as electromechanical transducers in electrohydraulic valves. This paper focuses on the investigations of two-layer piezo bending and piezo tube actuators used in electro hydraulic and electro pneumatic valves.

¹ Poznan University of Technology, Institute of Mechanical Technology, Poznan, Poland

* E-mail: andrzej.milecki@put.poznan.pl

<https://doi.org/10.5604/01.3001.0013.6235>

In the second part of the paper the Model Following Control and Fractional Order Control methods are presented. Their application for control of electrohydraulic servo drive is proposed and validated in laboratory experiments. The performed investigations results showed that the proposed control methods improved the servo drives dynamics.

2. APPLICATIONS OF PIEZOACTUATORS IN ELECTROHYDRAULIC VALVES

Micro-positioning tasks [1, 2], with assurance of high frequency of work are often important requirements for electrohydraulic and electro pneumatic valves. In such cases piezo actuators can be applied, because they are able to generate forces of kNs and they may work with frequencies ranging up to a few kHz. Such high resonance frequency of piezoelectric actuators enables them to drive a flapper in a first stage of servo valve. Two main types of piezo actuators i.e.: stack and bimorph actuators are available on a market. The first of them are linear actuators which can generate forces in a range of kNs with a displacement of a fraction of mm. These types of actuators must be supplied with controllable voltages in a range of kVs, which is a serious disadvantage. Bimorph actuator typically consists of one or two layers and can be used to bend, twist or elongate. When supplying, one layer expands while the other layer contracts. As a result the bending of the actuator is produced. The piezo bender actuators are able to generate forces to a few N and a motion in the range of fraction of millimetres. They can be supplied with low voltages equal to ± 100 V. Therefore, piezo bender actuators can be successfully applied in valves, requiring low forces.

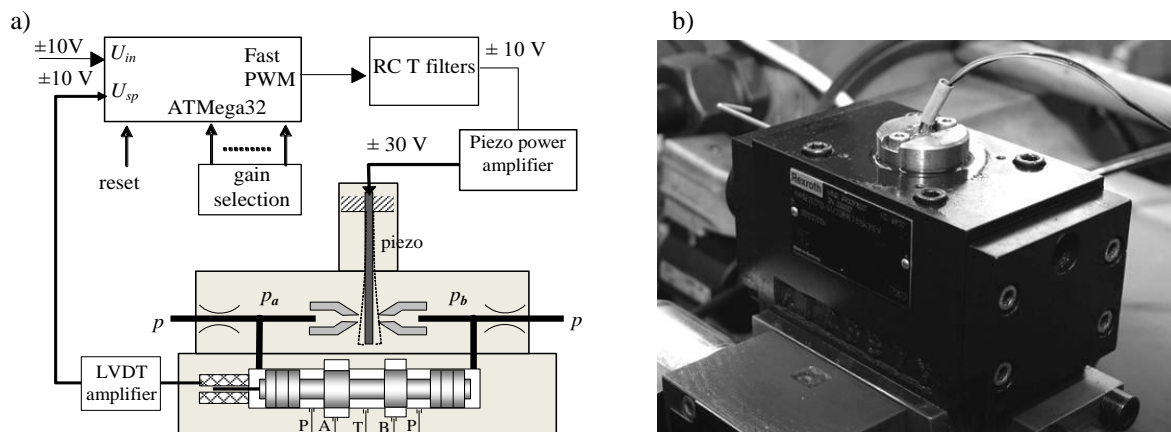


Fig. 1. The servo valve with piezo element: a) scheme, b) photo [3]

In the made at Poznan University of Technology investigations the torque motor in the servo valve is replaced by piezo bender actuator [3]. Its plate acts as a flapper placed between two nozzles (Fig. 1). To obtain the feedback, the application of spool displacement measure transducer, is used. Its output signal (spool position) is compared with assumed one and the control amplifier produces the voltage, to the piezo element. In presented here design, the piezo bender transducer type PL112.11 is applied [3]. It is characterized by displacement equal to $\pm 0,08$ mm, supplied by the maximum voltage equal to ± 30 V. Piezo element

generates the maximum output force equal to ± 2 N. In produced nowadays servo valves, torque motors with maximum torque from 20 mNm to 50 mNm are applied. For the flapper length of 20 mm, the generated by the torque motor force is from 1 N to 2.5 N. So, the torque motor can be replaced by piezo bender actuator. Neglecting the Coulombic and hydrodynamic forces the spool movement can be described as follows

$$\Delta p_m A_s = m_s \frac{d^2 x_s}{dt^2} + D_s \frac{dx_s}{dt} \quad (1)$$

where: m_s – the spool mass and moved working fluid (about 0.02 kg),

D_s – movement resistance coefficient (estimating: from 10 to 20 Nms).

The equation (1) can be converted to following transfer function

$$x_s(s) = \frac{k_{mp} \cdot A_s / D_s}{s \cdot \left(\frac{m_s}{D_s} s + 1 \right)} x_m(s) = \frac{k_m}{s \cdot (T_s \cdot s + 1)} x_m(s) \quad (2)$$

where: $k_m = (0.44 \div 0.88) \cdot 10^4$ 1/s – gain coefficient, T_s – time constant.

The time constant T_s can vary in dependence of movement resistance from 1 to 2 ms. In real valve some basic non-linear forces acts on the spool [4, 5] like the hydrodynamic and friction forces, which should be taken into account. Typically the friction force is rather low because the spool moves in oil, but it can increase significantly when in the oil contamination appears. The value of friction force can be only estimated. In the servovalve the maximum spool movement velocity is limited to about 1 m/s as a result of throttle flow saturation. The maximum displacements of the spool and the flapper are limited to ± 0.08 mm and to ± 0.5 mm, respectively. The hydrodynamic force can be linearized into following form

$$F_h = k_{hsl} \cdot x_s + k_{hdl} \cdot v_s \quad (3)$$

where: k_{hsl} , k_{hdl} – substitute gain coefficients.

In a static state the value of the first component depends mainly on spool position. In the dynamic states the second component begins to play more important role. It decreases the dynamic parameters of the valve.

Basing on presented above equations the model of servo valve with piezo actuator was created in Matlab-Simulink software. It is shown in Fig 2. In the model the simple hysteresis model and submodel of electrohydraulic single rod cylinder were added [6]. Typically, on servo valve control card input, the input signal ± 10 V is given. This voltage should cause the displacement of the spool within a range of ± 0.5 mm. It follows, that the measurement unit gain coefficient is equal to $k_{fm} = 10 \text{ V} / 0.00005 \text{ m} = 20\,000 \text{ V/m}$. Assuming that the designed servo valve will guarantee the maximum frequency 300 Hz, the throttles flow on nozzles inputs must guarantee achieving by the spool the necessary velocity. The displacement of the spool is equal to $x_{s\max} = \pm 0.5$ mm, which means that its maximum velocity should be equal to 0.9 m/s and the maximum acceleration will be equal to 1780 m/s^2 . For the spool diameter $d_s = 0.008$ m its cross section area is $A_s \approx 5 \cdot 10^{-5} \text{ m}^2$. It follows that achieving mentioned above spool velocity requires maximum flow equal to $2.7 \text{ dm}^3/\text{min}$ (average $1.9 \text{ dm}^3/\text{min}$). Supposing that spool mass equals $m_s = 0.02$ kg the required pressure difference on nozzles inputs can be calculated from the equation:

$$\Delta p_{\max} = m_s \cdot \ddot{x}_{s \max} / A_s \approx 0.71 \text{ MPa} \quad (4)$$

If the pressure difference $\Delta p_m = p_1 - p_2$ on nozzle's inlets depends only on flapper position the following equation governs the flapper-nozzle amplifier

$$\Delta p_m = \frac{\Delta p_{\max}}{x_{m \max}} x_m = k_{mp} x_m \quad (5)$$

where: $x_{m \max}$ – maximum flapper movement from central position,
 $k_{mp} \approx 8.9 \cdot 10^9 \text{ N/m}^3$ – coefficient.

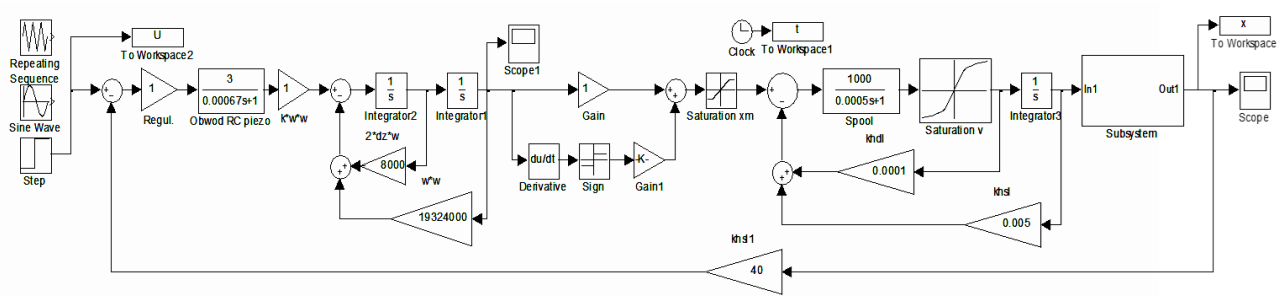


Fig. 2. The servo valve with piezo element simulation model

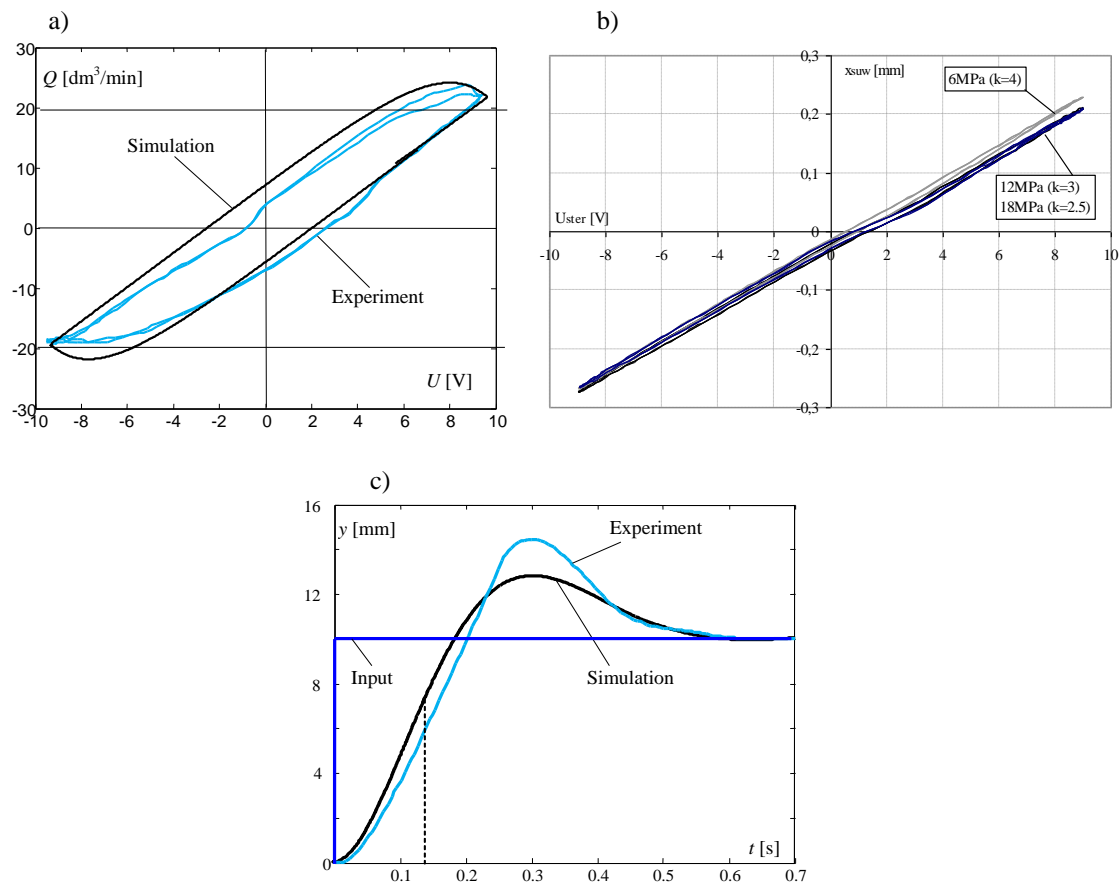


Fig. 3. Servo valve with piezoelectric bender actuator investigations results obtained in simulation and in laboratory experiments:

a) hysteresis of flow-supply voltage b) compensated hysteresis (spool displacement), c) servo drive step responses

The calculated above values of parameters are taken into simulation model shown in Fig. 2. The built valve (Fig. 1b) is installed on the test stand and investigated. The valve output flow changes obtained as a response of sinusoidal input signal, measured in simulation and investigation, are presented in Fig. 3a. In these curves significant hysteresis is visible, which is caused by piezo actuator hysteresis. Therefore in the next step the feedback control with P regulator is implemented, which reduced significantly the hysteresis (Fig. 3b). As a feedback signal the valve spool position is used. In Fig. 3c the obtained in simulation and in real investigations step responses of the electrohydraulic servo drive with the proposed valve with piezo bender actuator are shown. To control of the valve a simple P-type regulator is used. The investigated servo drive substitute time constant is about 0.13 s.

In another work made at PUT the PI Ceramic piezoelectric PT230 tube actuator supplied by voltage of $\pm 250\text{V}$ was investigated [7]. Depending on different electrical connection and electrodes configuration, the tube can change its radius dimension, bend the free end, and elongate along the longest axis. The geometrical parameters of the tube are: length $l = 40\text{ mm}$, outer diameter $d_o = 3.2\text{ mm}$, inner diameter $d_i = 2.2\text{ mm}$. This actuator was at first tested using sinusoidal signal with growing amplitude. The results are shown in Fig. 4, in which the relationship between input voltage and actuator displacement is shown. In the characteristic, the significant symmetric hysteresis of approximately 20% is visible.

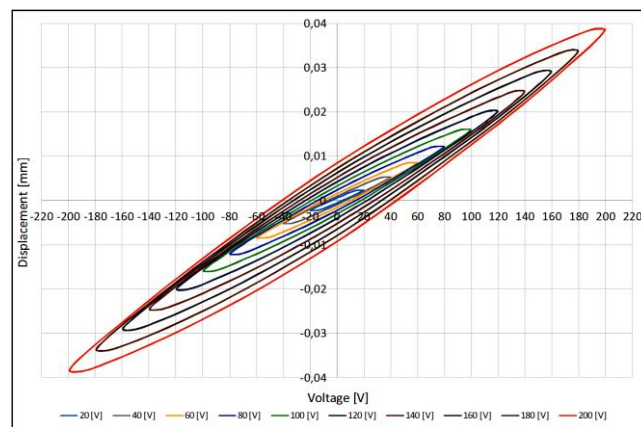


Fig. 4. The results of displacement for supply voltage for 3Hz sinus input signal with different amplitudes

In the next step of the research, the positioning control of the piezo tube actuator was proposed as shown in Fig. 5. In the research only two outer opposite electrodes were energized and the remaining electrodes were connected to the ground. The free end of the tube could bend along one axis. The feedback signal is generated by laser displacement sensor. The controller was implemented in Matlab Simulink environment. The classic PID-type control algorithm with positioning closed loop feedback was applied. This regulator was tuned manually under real time work in dSPACE software Control Desk. The results obtained in laboratory investigations have proven that the applied classical PID controller was effective and allowed the reduction of the hysteresis and thus the tracking error in a range of $\pm 1\mu\text{m}$.

The main idea of the research was to confirm the application possibility of the piezo tube actuator in pneumatic flapper-nozzle valve. At first the piezo tube was used to drive a single nozzle-flapper valve (see Fig. 6).

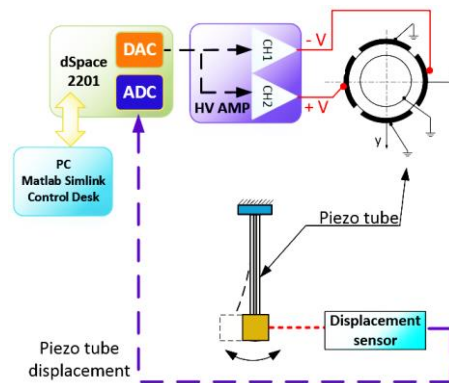


Fig. 5. Scheme of the test rig for feedback control

In the initial test, a mechanical flapper with position adjustment via micrometres screw was used. This test enabled to establish the pressure regulation range. In the second test, a piezo tube as a drive was used, to pressure control.

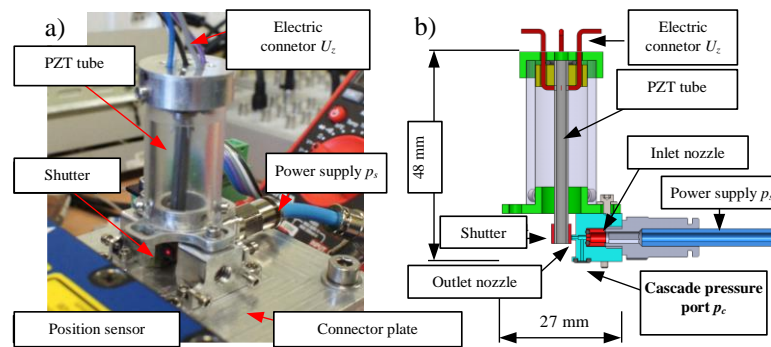


Fig. 6. The application of piezo tube in pneumatic valve: a) test stand photo, b) drawing

The tests were performed on test rig which scheme is presented in Fig. 7. The air is delivered by the inlet orifice to the cascade chamber. In the investigations two control voltages $+U_z$ and $-U_z$ are generated by the supply unit. The maximum air pressure was 0.6 MPa, and the maximum piezo voltage supply was set up to 200 VDC.

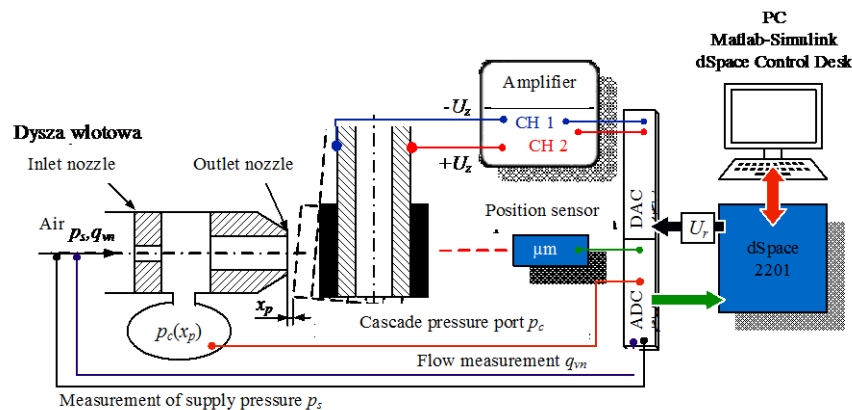


Fig. 7. The test stand structure

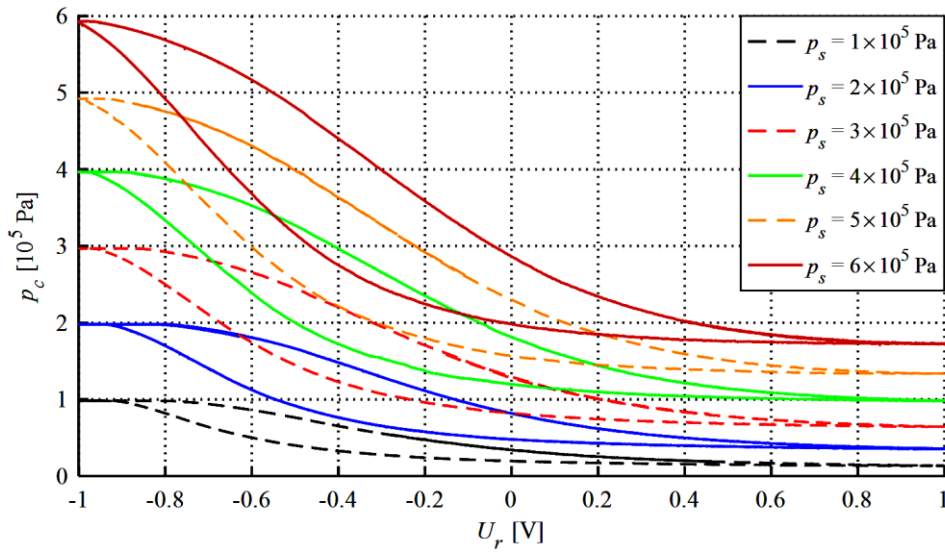


Fig. 8. Investigation results

In the test stand shown in Fig. 7 an orifice with inlet diameter 0.22 mm and outlet diameter 0.34 mm was used. The measured quasi-static characteristic of the valve driven by piezo flapper are shown in Fig. 8, in which the control pressure $p_c(x_p)$ changes for different supply pressures are presented. The actuator was able to almost fully close the outlet orifice, thus the maximum control pressure was $p_{c \max} = 5.94 \cdot 10^5$ Pa, which was almost the same as supply pressure. Similar results were obtained for other supply pressures. However, if the nozzle was full opened, due to low diameter of the outlet orifice, the control pressure p_c was not equal to atmospheric pressure. The range of pressure changes was $85.4\% \cdot p_s$ for supply pressure $p_s = 0.6$ MPa and $77.4\% \cdot p_s$ for supply pressure $p_s = 0.3$ MPa.

In Fig. 9 the pneumatic valve with two nozzles and a flapper driven by piezo tube is presented. The valve static characteristics i.e. the controlled output pressure as a function of control voltages $p_c(U_r)$ are shown in Fig. 10.

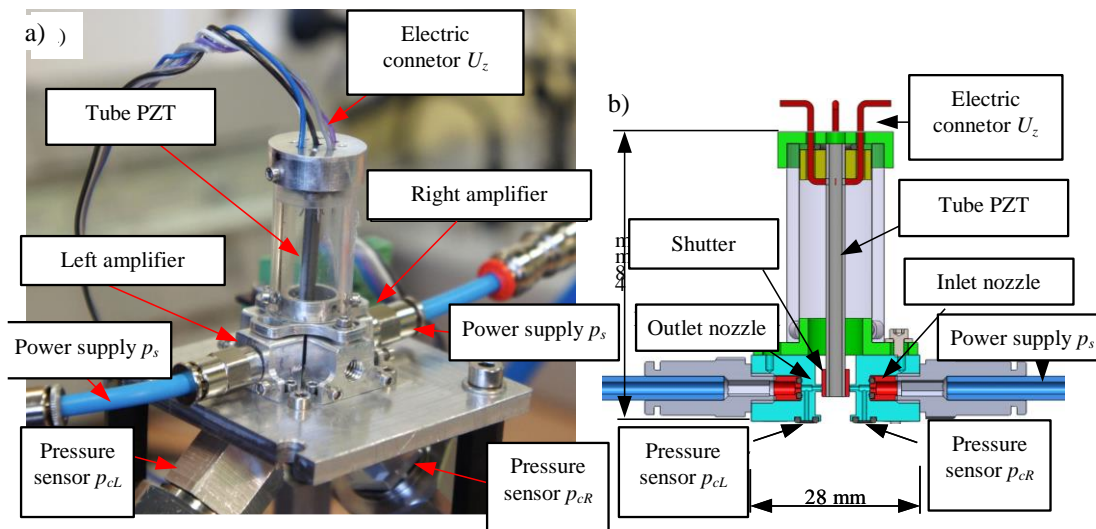


Fig. 9. The test stand photo (a) and drawing (b) for two nozzles

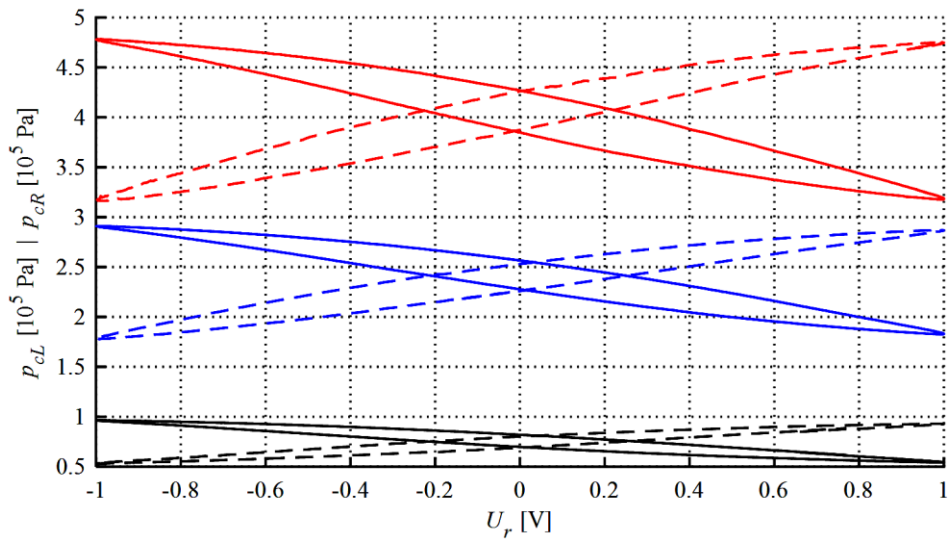


Fig. 10. Investigations results

The investigated valve is characterized by hysteresis. For supply pressure $p_s = 0.5$ MPa its max value is 43%; its middle value for $p_s = 0.3$ MPa is 22%. The solid line shows the control pressures $p_{cL}(U_r)$ in left nozzle and the dashed line shows control pressures $p_{cR}(U_r)$ in right nozzle.

3. MODEL FOLLOWING CONTROL (MFC) OF ELECTROHYDRAULIC DRIVE

The MFC method derived from the idea of Model Based Control [8, 9], in which the part of the control system structure is a simulation model of the controlled process or object. The block structure of classic MFC system is shown in Fig. 11.

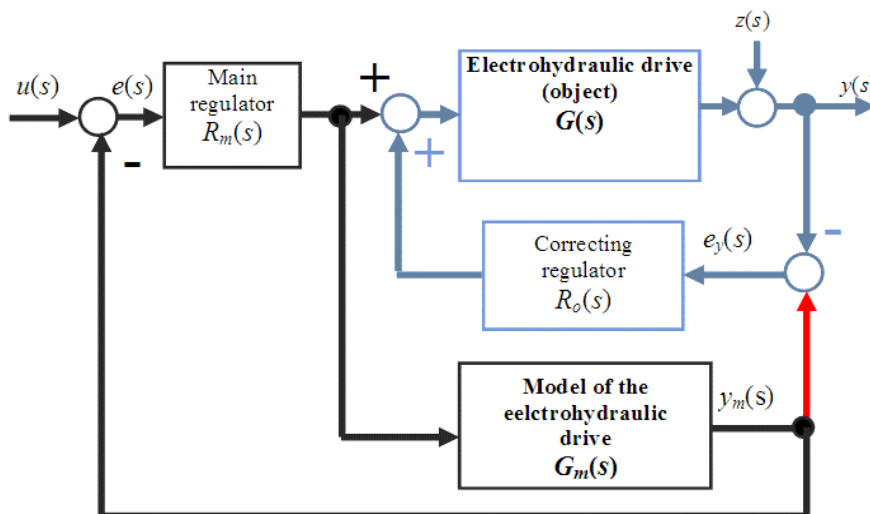


Fig. 11. The Model Following Control block scheme

It appeared in the literature in the early 1990s. In the MFC method, the control bases on two regulators: $R_m(s)$ and $R_o(s)$. The first one controls directly the model of the object $G_m(s)$ and partially the real object, which in described here case, is the electrohydraulic drive, described by transfer function $G(s)$. The real object is additionally controlled by the second regulator, which input signal is the difference between the real object output signal and the object model output signal. By this way this controller $R_o(s)$ corrects the real drive i.e. its inaccuracies and disturbances. There is assumed in the MFC method, that the object model $G_m(s)$ is a pattern for the control. In the MFC concept two loops may be distinguished: the model loop R_m-G_m and the real object loop R_o-G . The first loop (marked by black color in Fig. 13) consists of the model of a controlled object and the linear controller type PID. The difference between the output signal of the model y_m and the output signal of the real object y is used by regulator for the calculation of real object control signal correction. The model of the object is usually identified by a mathematical analysis or by experimental tests. The regulator $R_m(s)$ used in the process loop for generation of the object control signal, uses the error signal which is calculated as the difference between the assumed signal u and the model output signal y_m . The system output signal can be calculated using following equation

$$y_{MFC}(s) = \frac{R_m(s)G_m(s)G(s)[1 + R_o(s)G_m(s)]}{[1 + R_m(s)G_m(s)]G_m(s)[1 + R_o(s)G(s)]} u(s) + \frac{1}{1 + R_o(s)G(s)} z(s) \quad (6)$$

where: $u(s)$ – input signal, $y(s)$ – output signal, $z(s)$ – disturbances, $G(s)$ – controlled object, $R_o(s)$ – object controller, $G_m(s)$ – object model, $R_m(s)$ – model controller.

The MFC controller was implemented on typical PLC. The scheme of this implementation is shown in Fig. 12 [10]. Two digital PID controllers are used. The PLC is connected to the electrohydraulic servo drive by AD and DA converters, using PLC IN and PLC OUT ports.

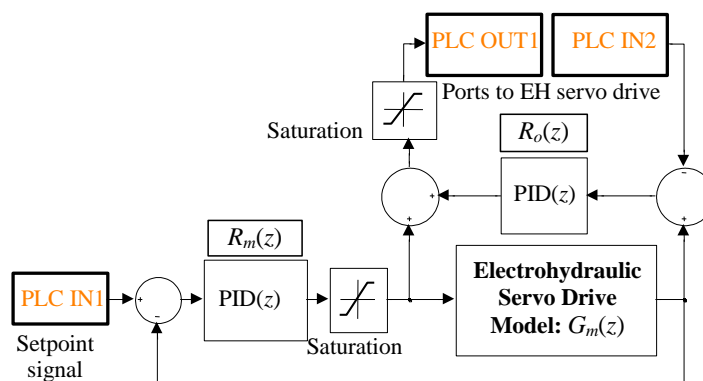


Fig. 12. Control system implemented on PLC

In order to match the signals from the PLC to the electrohydraulic valve card and cylinder displacement sensor two saturation blocks are used. The rapid prototyping technique was used for MFC control system design and implementation. In this way, the model of the control system has been built previously in software environment and recompiled for the C

code and then, implemented as one of the task class, in the PLC CPU unit. Due to the discrete work of the industrial controller, it was required to discretize the continuous model of control system, therefore also the Electro Hydraulic Servo Drive model is discretized. In the investigations both PID and MFC control system of electrohydraulic servo drive was tested by analysing step responses signal. The parameters of both PID controllers used in the MFC method were established experimentally as follows: $k_p = 15$, $k_i = 0.001$, $k_d = 0.005$. In order to achieve the improvement of controlled drive dynamics, the gain coefficient k_p of $R_o(s)$ controller was gradually increased from 15 to 60. In order to assess the results obtained if the MFC controller is used, the same investigations were made but with the use of simple PID controller, which parameters are the same as mentioned above. The results are shown in Fig. 13. The achieved settling time was 1.6 s if PID control is used, and about 1.0 s for MFC control method. This result confirmed the sense of MFC control application.

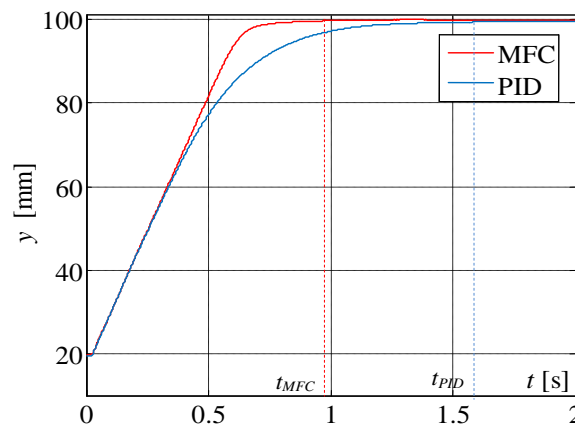


Fig. 13. The step responses of the electrohydraulic servo drive

4. FRACTIONAL ORDER CONTROLLER APPLICATION

A classical PID controllers are currently most widely used in industrial applications. This concerns also the electrohydraulic servo drives. However, there is still important to find better solutions in order to improve both, the dynamics and positioning accuracy. In last few years a fractional order controllers became interesting and several investigations have been undertaken in different areas of engineering. Therefore the investigations made at PUT are focused on application of fractional order PI controller in positioning of an electro-hydraulic drive with Bosh Rexroth proportional valve. Fractional differential-integral equation can be written as follows [11]:

$${}_a D_t^\alpha = \begin{cases} \frac{d^\alpha}{dt^\alpha} & \alpha > 0 \\ 1 & \alpha = 0 \\ \int_a^t (dr)^{-\alpha} & \alpha < 0 \end{cases} \quad (7)$$

where: a and t are the limits of the integration operation and α (real number) is the order of derivation.

The equation, describing the transformation of the Laplace operator of fractional differentiation row for zero initial conditions is defined as:

$$L[D_t^\alpha f(t)] = s^\alpha F(s) \tag{8}$$

In practice, the fractional order controller must be implemented in real hardware and software environment. To this end this controller should be approximated by ordinary differential equation. In most cases the Oustaloup method, described in detail in [10] is applied. The formula is defined as follows:

$$s^q = k \prod_{n=1}^N \frac{1 + \frac{s}{\omega_{zn}}}{1 + \frac{s}{\omega_{pn}}} \quad q > 0 \tag{9}$$

In this equation the parameters are defined as follows:

$$a = \left(\frac{\omega_h}{\omega_l}\right)^{\frac{q}{N}}, \quad \eta = \left(\frac{\omega_h}{\omega_l}\right)^{\frac{1-q}{N}}, \quad \omega_{zn} = \omega_{p,n-1}\eta \quad n=2, \dots, N \text{ and } \omega_{pn} = \omega_{z,n-1}a \quad n=1, \dots, N.$$

where: q – the fractional order (real number), k – gain coefficient, adjusted so, that both sides have unit gains at 1 rad/s, N – order of the finite transfer function approximation, ω_l – low frequency limit, ω_h – upper frequency limit.

The first goal was to implement this controller on the Programmable Logic Controller platform, working under real time operating system Automation Runtime. The user interface was built using the touch panel. Continuous transfer function taken from the Oustaloup calculations, can be directly implemented on the controller like PLC. PLC input and output modules are connected via Powerlink interface. This interface provided transmission speed of 100Mbit/s. The controller is connected using analog input module to the magnetostrictive sensor built in hydraulic cylinder used for position measurement. Analog PLC output module was connected to the proportional valve control card (Fig. 14).

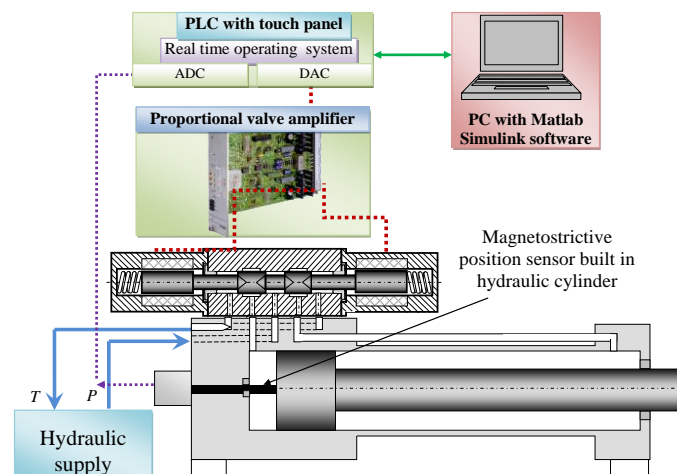


Fig. 14. The scheme of control stand

The investigation results are presented in Fig. 15, in which the step responses of the electrohydraulic servo drive controlled by typical PI controller and by FO PI controller are shown. In the first case the substitute time constant was 0.14 s and in a second case it was 0.08 s, which shows dynamics improvement if the drive is controlled by FO PID.

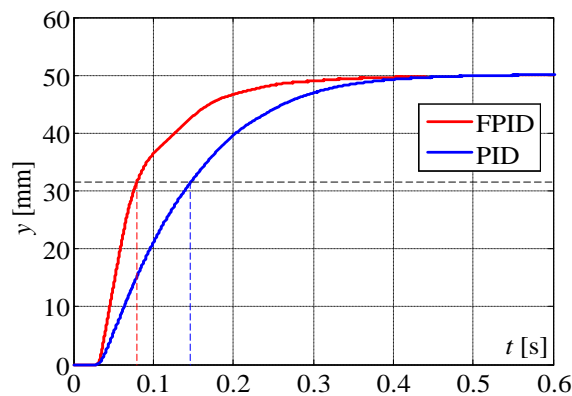


Fig. 15. The step responses of the electrohydraulic servo drive

5. CONCLUSION / SUMMARY

In the paper the investigations the piezo bender actuator application in servo valve are presented. The simulation model of such modified valve was proposed and implemented in Matlab-Simulink. The built valve is characterised by significant hysteresis, which was reduced by application of closed loop PID control. The application of piezo tube actuator as a flapper in pneumatic valve is also proposed and investigated. The investigation results have shown that the both hydraulic and pneumatic flapper-nozzle valves with piezo actuators assured the obtainment of usable pressure changes. In the article, also the applications of Model Following Control and Fractional Order Control methods in electro-hydraulic drive are described. The performed investigations have shown, that the application of these methods enabled the improvement of drive step response time.

ACKNOWLEDGEMENTS

This work was supported by Polish Ministry of Science and Education grants No. 02/22/SBAD/1501.

REFERENCES

- [1] TSENGA A.A., NOTARGIACOMOB A., CHEN T. P., 2005, *Nanofabrication by scanning probe microscope lithography*, Journal of Vacuum Science and Technology, 23, 877–894.
- [2] RUBIO-SIERRA F. J., HECKLE W. M., and STARK R. W., 2005, *Nanomanipulation by atomic force microscopy*, Advanced Engineering Materials, 7/4, 193–196.
- [3] SEDZIAK D., REGULSKI R., 2015, *Design and Investigations into the Piezobender Controlled Servovalve*, Solid State Phenomena, 220–221, 520–525.

- [4] WALTERS R.B., 2014, *Hydraulic and Electro-Hydraulic Control Systems*, Springer Netherlands.
- [5] HERAKOVIC N., 2009, *Flow-Force Analysis in a Hydraulic Sliding-Spool Valve*, *Strojarstvo* 51/6 555–564.
- [6] MILECKI A., 2005, *Simulation investigations of servovalve with piezo bender actuator*, *Hydraulika a Pneumatika*, 3–4, 57–60.
- [7] REGULSKI R., STEFAŃSKI F., MINOROWICZ B., SĘDZIAK D., 2015 *Research of Basic Parameters of Piezoelectric Tube Actuator*, *International Conference on Automation,; Progress in Automation, Robotics and Measuring Techniques*, 275–281,
- [8] TYLER, J. S., Jr., 1964, *The Characteristics of Model Following Systems as Synthesized by Optimal Control*, *IEEE Trans. Automatic Control*, 9/4, 485–498.
- [9] ERZBERGER H., 1968. *On the Use of Algebraic Methods in the Analysis and Design of Model-Following Control System*, NASA TN D-4663.
- [10] MILECKI A., RYBARCZYK D., OWCZAREK P. 2014, *Application of the MFC Method in Electrohydraulic Servo Drive with a Valve Controlled by Synchronous Motor*, *Recent Advances in Automation, Robotics and Measuring Techniques. Advances in Intelligent Systems and Computing*, 267. Springer International Publishing, 167–174.
- [11] CHEN Y., PETRAS I. and XUE D. 2009, *Fractional order control – a tutorial*, In: *Proceedings of American Control Conference*, Hyatt Regency Riverfront, St. Louis, USA, 2009, 1397–1411.
- [12] RYBARCZYK D., 2017, *Use of the fractional order PD controller in electro-hydraulic drive*, *PAR* 1/2017, DOI: 10.14313/PAR_223/13, 13–18.